journal

J. Am. Ceram. Soc., 87 [6] 1047–1052 (2004)

Effect of V_2O_5 Doping on the Sintering and Dielectric Properties of *M*-Phase $Li_{1+x-y}Nb_{1-x-3y}Ti_{x+4y}O_3$ Ceramics

Albina Y. Borisevich*,† and Peter K. Davies**

Department of Materials Science and Engineering, University of Pennsylvania, Philadelphia, Pennsylvania 19104-6272

The effect of the addition of V_2O_5 on the structure, sintering and dielectric properties of *M*-phase ($Li_{1+x-y}Nb_{1-x-3y}Ti_{x+4y}O_3$) ceramics has been investigated. Homogeneous substitution of V^{5+} for Nb^{5+} was obtained in $LiNb_{0.6(1-x)}V_{0.6x}Ti_{0.5}O_3$ for $x \leq 0.02$. The addition of V_2O_5 led to a large reduction in the sintering temperature and samples with $x = 0.02$ could be fully densified at 900°C. The substitution of vanadia had a relatively minor adverse effect on the microwave dielectric properties of the *M*-phase system and the $x = 0.02$ ceramics had $\varepsilon_r = 66$, $Q \times f = 3800$ at 5.6 GHz, and $\tau_f = 11$ ppm/°C. Preliminary investigations suggest that silver metallization does not diffuse into the V_2O_5-doped *M*-phase ceramics at 900°C, making these materials potential candidates for low-temperature cofired ceramic (LTCC) applications.

I. Introduction

Low-temperature cofired ceramics (LTCC) are receiving increased attention in the research community because of their potential for novel multilayer communication modules involving the integration of passive components. The major requirements for these materials are sinterability below the Ag/Cu metallization melting temperature (≈900°C), chemical compatibility with the metallization material within the temperature and time scale of the sintering process, as well as good microwave properties. Three classes of LTCC compositions have been investigated.[1] The first includes "low-fire materials," generally Bi-based, such as Bi pyrochlores (e.g., Ref. 2) and sillenites (e.g., Ref. 3). The second type includes glass-ceramic composites with high glass contents (~45%). These two approaches are combined in the third class, which uses ceramics with relatively low sintering temperatures (1100°–1150°C) and small amounts of glass or sintering aids (e.g., Ref. 4). This paper reports on a new family of low-sintering temperature dielectric compositions based on the *M*-phase $Li_{1+x-y}Nb_{1-x-3y}Ti_{x+4y}O_3$ system.

The so-called *M*-phase compounds in the Li_2O–Nb_2O_5–TiO_2 system were first reported by Villafuerte-Castrejon *et al.*[5] as forming a solid solution, $Li_{1+x-y}Nb_{1-x-3y}Ti_{x+4y}O_3$, with $0.05 \leq x \leq 0.3$, $0 \leq y \leq 0.182$. Recent studies of the structure of the *M*-phase system[6,7] have shown it is best described as a homologous series of compounds with a layered structure comprised of $LiNbO_3$-type (LN) blocks separated by single corundum-type $[Ti_2O_3]^{2+}$ layers. The charge of the layers is compensated by partial Ti^{4+}/Nb^{5+} substitution within the LN blocks. The thickness of the LN block, which is determined by the Ti content, varies from 4 (at the Ti-rich end) to ~50 cation layers (at the $LiNbO_3$-rich end).

The microwave dielectric properties of the *M*-phase system have also been investigated.[6] The relative permittivity ranged from 78 at the LN-rich end of the system to 55 for the Ti-rich compositions. All of the phases exhibited good Q values in the microwave region with the value of $Q \times f$ approaching 9000. The temperature coefficient of resonant frequency τ_f changed sign from negative (for $LiNbO_3$-rich compositions) to positive (Ti-rich compositions) with a zero value in the intermediate region. Because those studies also showed that the *M*-phase $Li_{1+x-y}Nb_{1-x-3y}Ti_{x+4y}O_3$ system could be sintered to essentially full density at relatively low temperatures, 1100°–1150°C, additional investigations were initiated to identify methods for reducing their sintering temperature to a range appropriate for LTCC applications.

V_2O_5 was chosen as a candidate sintering aid because of its low melting point (680°C) and the chemical similarity of V^{5+} to Nb^{5+}. The choice of V_2O_5 was also guided by its successful application in lowering the sintering temperatures of several other niobate (e.g., $SrBi_2Nb_2O_9$[8]) and titanate (e.g., $BaBi_4Ti_4O_{15}$[9]) ceramic compositions. While a certain degree of homogeneous V^{5+}/Nb^{5+} substitution in the *M*-phase is possible, differences in ionic radii and the potential formation of compounds with reduced oxidation states usually preclude complete compatibility and often result in low solid solubilities of V-based compounds in their Nb analogues. For example, the structure of $LiVO_3$ is very different from that of $LiNbO_3$ and contains tetrahedrally coordinated V^{5+} ions;[10] similarly, solid solution of $LiVO_3$ in $LiNbO_3$ can be obtained only at high pressure.[11] Thus it was expected that any solid solubility of V^{5+} in *M*-phase would be very limited.

The present study details the results on the effect of the addition of V_2O_5 on the structure, sintering, and dielectric properties of the niobate *M*-phases and explores their compatibility with Ag metal. $LiNb_{0.6}Ti_{0.5}O_3$, which has a τ_f close to zero, was chosen as the base composition.

II. Experimental Procedure

The samples for the dielectric property measurements were prepared from dried powders of Li_2CO_3 (Baker, 99.0%), Nb_2O_5 (Cerac, 99.95%), TiO_2 (Cerac, 99.9%), and V_2O_5 (Baker, 99.6%). The mixing ratio was chosen to give the desired level of substitution of Nb by V according to the formula $LiNb_{0.6(1-x)}V_{0.6x}Ti_{0.5}O_3$, where x ranged from 0.01 to 0.05. After mixing under acetone, the powders were preannealed at 600°C to expel CO_2 while avoiding melting V_2O_5, reground, and annealed between 800°C ($x = 0.05$) and 900°C ($x = 0.01$) for 6 h in air. One treatment was sufficient to obtain a product with no secondary phases detectable by X-ray diffraction (collected on a Rigaku DMaxB diffractometer using Cu$K\alpha$ radiation generated at 45 kV and 30 mA). After ball milling in ethanol the single-phase powders were isostatically pressed into pellets at 0.56 GPa and annealed for 1 h in air at 825°C ($x = 0.05$) to 925°C ($x = 0.01$). During the sintering the pellets were buried

D. W. Johnson Jr.—contributing editor

Manuscript No. 10428. Received July 31, 2003; approved March 5, 2004.

This work was funded by the National Science Foundation (Grant No. DMR 02-13489) and made use of the MRSEC shared experimental facilities supported by the National Science Foundation through Grant No. DMR 00-79909.

*Member, American Ceramic Society.

**Fellow, American Ceramic Society.

†Current address: Condensed Matter Sciences Division, Oak Ridge National Laboratory, Oak Ridge, Tennessee 37831-6031.

in sacrificial powder of the same composition. The sintered ceramics were light brown with the shade intensifying with V content, and their density was between 94% and 98% of the theoretical value. Electron spin resonance spectra of selected powders were acquired using a Bruker ESP-300 spectrometer in the field range chosen to include the reported values for V^{4+} (Ref. 12) and Ti^{3+} (Ref. 13) ions in a similar coordination.

The relative permittivity, ε_r (calculated from the capacitance assuming room-temperature dimensions), and dielectric loss tangent, tan δ, were measured in the 100 Hz to 1 MHz frequency range from −100° to 200°C by the parallel-plate method using an HP 4284A precision LCR meter and a Delta 9920 environmental chamber. The temperature coefficient of capacitance τ_c was calculated for −20° to 80°C from linear fits of the permittivity data. Microwave measurements were performed via the cavity reflection method using an HP 8719C network analyzer. Ceramic cylinders with a height-to-diameter ratio of ~0.4 were placed into a gold-plated resonant cavity, and their permittivities and *Q* values were calculated at the resonant conditions from the S_{11} reflection coefficients. The temperature coefficient of the resonant frequency (τ_f) was determined in the temperature range 0°–80°C by inserting the test cavities into a temperature-controlled chamber. The setup and methodology are described in detail in Ref. 14.

To investigate the compatibility of the ceramics with silver metal the $x = 0.02$ powders were processed to give an average particle size of 0.87 μm. Pellets were pressed as described above and coated with silver paste (Heraeus ST1601-14). After a 15 min treatment at 530°C to expel volatile components in the silver paste, the compact was heated for 1 h at 900°C.

The SEM studies were conducted at 20 kV using a JEOL 6300F scanning electron microscope equipped with a PGT energy dispersive X-ray detector. Specimens for TEM/STEM studies were prepared from pellets by conventional polishing, dimpling, and ion milling. To eliminate the possibility of water leaching any of the unreacted components, all polishing, slicing, etc., were conducted with kerosene as a lubricant with subsequent washing in hexane. Specimens were examined at 200 kV using a JEOL 2010F microscope equipped with a PGT energy dispersive X-ray detector.

III. Results and Discussion

For the phase analysis studies, samples were formulated for 1%–5% substitution of Nb by V in $LiNb_{0.6}Ti_{0.5}O_3$ ($LiNb_{0.6(1-x)}V_{0.6x}Ti_{0.5}O_3$ with $x = 0.01$ to 0.05), processed as described in Section II, and then annealed at 1000°C to obtain higher-quality XRD patterns by increasing the grain size. Pure $LiNb_{0.6}Ti_{0.5}O_3$ could be indexed as a single-phase $N = 10$ structure with $a = 5.1254(4)$ Å, $c = 23.207(2)$ Å, where *N* represents the superstructure periodicity.[6,7] Because the value of *N* was previously shown to be primarily determined by the Ti content (*N* decreases as the Ti content increases), no change would be expected for the isovalent substitution of Nb by V. The cell parameters of $LiNb_{0.6(1-x)}V_{0.6x}Ti_{0.5}O_3$ with $x = 0-0.02$ all gave an excellent fit to the $N = 10$ structure; the *a* parameter decreased with increasing *x*, while *c* showed no detectable change (see Fig. 1(a)). These cell parameters are consistent with the expected behavior of a homogeneous solid solution and reflect the decrease in the average ionic radii in the $LiNbO_3$-type blocks due to the smaller size of V^{5+} (0.54 Å) compared with Nb^{5+} (0.64 Å).[15]

The diffraction patterns of samples with $x = 0.03$ to 0.05 could no longer be accurately indexed by the $N = 10$ cell, and the errors in the cell parameter refinement were unrealistically high. Therefore, the X-ray diffraction patterns of these samples were indexed using a variable value of *N* (see details in Ref. 6). The variable periodicity model allowed the XRD patterns of all the V_2O_5-doped samples to be indexed satisfactorily. The data for the average superstructure periodicity are presented in Fig. 1(b). The value of $\langle N \rangle$ is constant (10) for $x = 0$ to 0.02 and then increases steeply for more V-rich compositions, reaching 10.8 for $x = 0.05$. From the correlations observed previously for these systems, an increase in the average periodicity reflects a decrease in the overall Ti content in the *M*-phase. This would imply that for the higher V concentrations some of the Ti content is incorporated into a second phase that could not be detected by XRD, presumably because of its small volume fraction or its amorphous character. The results of the lattice parameter refinements support a very narrow range of solid solubility in the $LiNb_{0.6(1-x)}V_{0.6x}Ti_{0.5}O_3$ system with the limit lying between $x = 0.02$ and 0.03 at 1000°C.

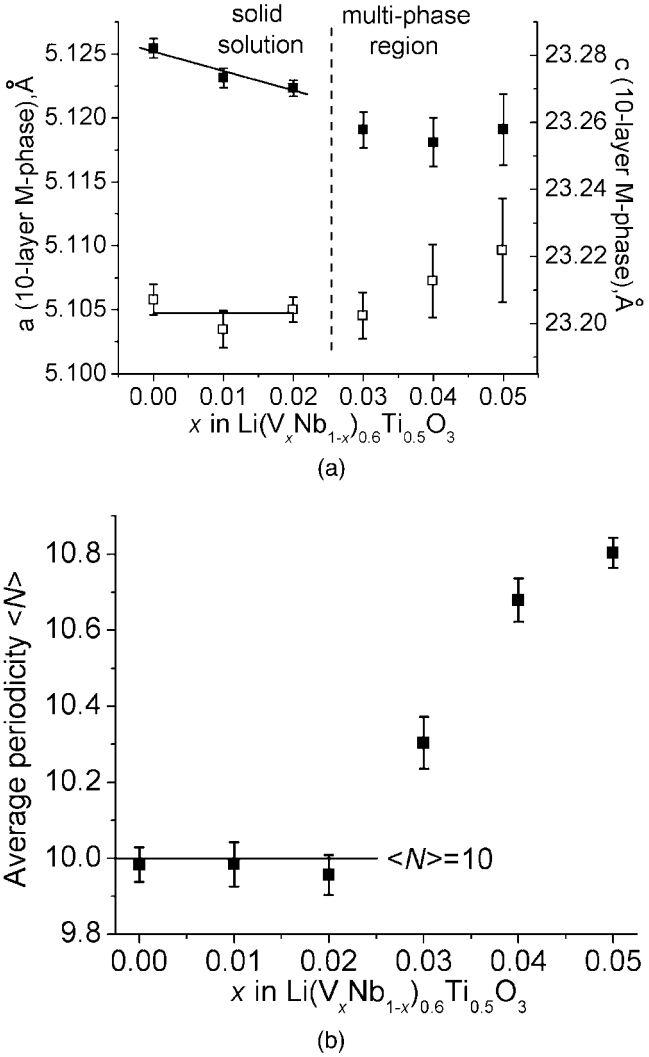

Fig. 1. Lattice parameters of $Li(Nb_{1-x}V_x)_{0.6}Ti_{0.5}O_3$ powders versus doping level (*x*): (a) *a* (filled dots) and *c* (open dots) lattice parameters calculated for $N = 10$ *M*-phase cell, (b) *M*-phase superstructure periodicity $\langle N \rangle$ (see text).

While many reduced compounds of V are stable, the light coloring of the samples and their low dielectric loss (and hence low conductivity; see below) was consistent with V remaining in the +5 state. This speculation was confirmed by an ESR investigation of the $x = 0.02$ powder, which showed no evidence for reduced forms of V or Ti.

The sintering properties of the V-doped samples were investigated on compacts prepared from prereacted (at 800°–900°C) single-phase powders. The sintering temperature was defined as the lowest temperature that achieved a density of >90% of the theoretical value after 1–2 h heat treatment. The sintering temperature decreased rapidly with the addition of V_2O_5 (Fig. 2), and for $x = 0.02$ the samples could be densified at 900°C.

Data for the dielectric properties of the sintered pellets at 1 MHz are shown in Fig. 3. The permittivity decreases linearly with increasing V content while the temperature coefficient of capacitance is nonmonotonic and is apparently affected by the transition

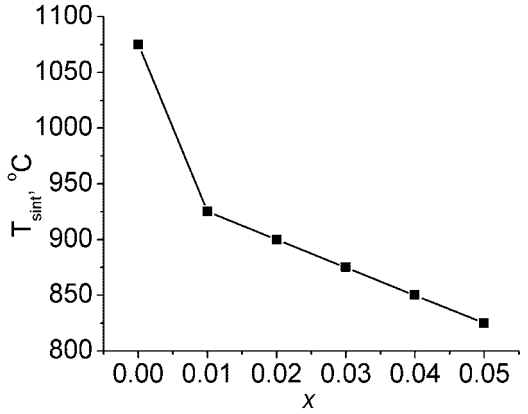

Fig. 2. Sintering temperature of $Li(Nb_{1-x}V_x)_{0.6}Ti_{0.5}O_3$ ceramics versus doping level (x).

from a single-phase ($x = 0$ to 0.02) to multiphase mixture ($x = 0.03$ to 0.05). The measured dielectric loss tangent at 1 MHz was negative, indicating that the precision of the measurement was not high enough to determine the actual loss. The values and trends in the relative permittivity at microwave frequencies were in good agreement with the 1 MHz data (Table I). The observed $Q\times f$ values generally decreased with doping level, with the sharpest drop coinciding with the initial introduction of V. The temperature coefficient of resonant frequency behaved irregularly with the level of substitution, although the observed values were quite low for most of the samples. Overall, the system shows excellent promise as a low-sintering microwave dielectric material and, for example, for the $x = 0.02$ sample ($T_{sint} = 900°C$) $\varepsilon_r = 66$, $Q\times f = 3800$ (5.6 GHz), $\tau_f = 11$ ppm/°C. It should also be noted that by modifying the composition of the undoped starting material, completely temperature compensated low sintering ceramics would be possible.

The compatibility of the V-doped system with Ag metallization under the sintering conditions was also examined. While several stable phases are known in both the Ag_2O–Nb_2O_5[16] and Ag_2O–V_2O_5[17] binaries, the reactivity of a complex compound such as the *M*-phase system cannot be predicted from this data. Preliminary investigations were made by examining the XRD patterns of Ag + V-*M*-phase ($x = 0.02$) composites before and after sintering at 900°C for 2 h. No third-phase peaks were observed after the thermal treatment (Fig. 4(a)), suggesting that the doped material is compatible with silver metal under the sintering conditions.

A more detailed study was conducted using a pressed compact of prereacted $x = 0.02$ V-*M*-phase powder. A silver electrode was applied to the green body, which was then sintered at 900°C. Figure 4(b) shows an SEM micrograph of the cross section of the

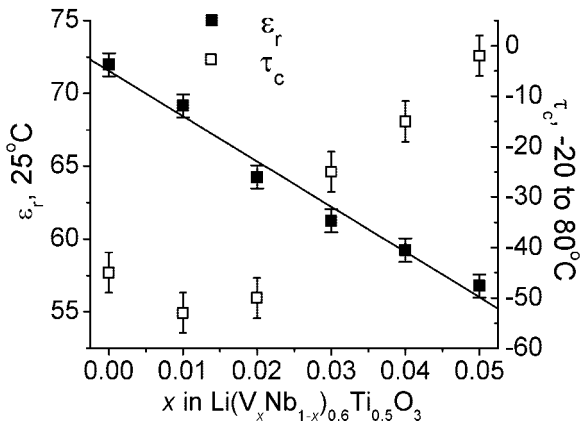

Fig. 3. Relative permittivity (filled dots) and temperature coefficient of capacitance (open dots) of $Li(Nb_{1-x}V_x)_{0.6}Ti_{0.5}O_3$ ceramics at 1 MHz.

Table I. Microwave Dielectric Properties of $Li(Nb_{1-x}V_x)_{0.6}Ti_{0.5}O_3$

x	f (GHz)	ε_r	$Q\times f$ (GHz)	τ_f (ppm/K)
0	5.66	65	6400	+8
0.01	5.41	66	3000	+40.5
0.02	5.55	66	3800	+11
0.03	5.61	64	2500	+15.5
0.04	5.48	64	1900	+12
0.05	5.74	59	1000	+43

final product. Compositional imaging using an EDX microprobe (not shown) allowed us to identify a layer denoted as I as Ag metallization. The interface between metallization layer I and ceramic layer II is quite sharp, suggesting good compatibility. Image contrast associated with the top part of the ceramic layer (IIa) is similar to that of the metallization; however, no traces of Ag were detected by EDX below the I–II interface. The contrast likely arises from the interaction of the ceramic with the glass frit or organic components of the paste, as the thickness of the IIa layer depends strongly on the curing treatment of the silver metallization; the exact changes in the ceramic have not been determined. The results of the experiment nevertheless appear promising as there is no Ag diffusion across the interface. It is also possible that a fully compatible metallization could be found by varying the corresponding glass/organic additives.

The amount of V_2O_5 required to achieve a significant reduction in the sintering temperature of the *M*-phase is very small, and does not induce any significant deterioration in the dielectric response. The most likely explanation for the reduction in the densification temperature is that the sintering is assisted by liquid-phase transport across the grain boundaries. This explanation would be consistent with the melting point of V_2O_5, which is lower than the sintering temperature. This mechanism generally manifests itself through the formation of liquid inclusions in the grain boundaries and triple points. A study of the microstructure was conducted to find direct evidence for a liquid-phase-assisted mechanism. The $x = 0.02$ composition was used for the study as it exhibits the most promising dielectric properties. SEM analyses revealed no evidence for liquid-phase formation perhaps due to the limited resolution of this technique or the difficulty in the observation of the associated features on the surface of a thick specimen. Therefore, further observations were made on thinned specimens using TEM/STEM.

To maximize the potential role of a liquid-phase sintering mechanism a new sample was made in which V_2O_5 was added to preformed *M*-phase samples of $LiNb_{0.6}Ti_{0.5}O_3$. The sample was prepared from ball-milled powders of $LiNb_{0.6}Ti_{0.5}O_3$ with a comparatively large grain size, mixed with V_2O_5 powder to give the same weight percentage of V_2O_5 (0.82%) as in the previously prepared $x = 0.02$ samples.[‡] A series of pellets prepared from this mixture were annealed at 900°C for 0 to 80 min, characterized by X-ray diffraction, and examined by TEM and STEM. The sintering proceeded rapidly, though the highest density (84%) achieved after annealing this composite for 80 min is somewhat lower than those (91%–95%) obtained after a 1 h treatment of the prereacted $x = 0.02$ powder. This decrease can be attributed to the difference in grain size.

The microstructure study provided evidence for liquid inclusions in all of the investigated samples. Figure 5(a) shows an example of a liquid-phase layer wetting a grain boundary in a sample sintered for 30 min. The small thickness of the layer (~30 nm) is consistent with the observation that very small amounts of additive are effective in improving the density. EDX microprobe analysis of this and other similar features clearly demonstrated a

[‡]Although the bulk composition of this sample is somewhat different from that of $x = 0.02$, it is very close, and corresponds to $Li_{0.989}Nb_{0.607}Ti_{0.494}O_3$ composition within the *M*-phase field with 2.2% V/Nb substitution.

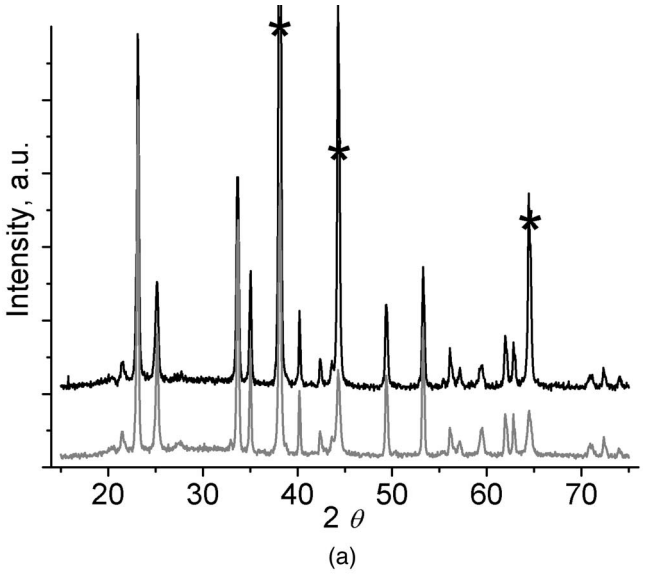

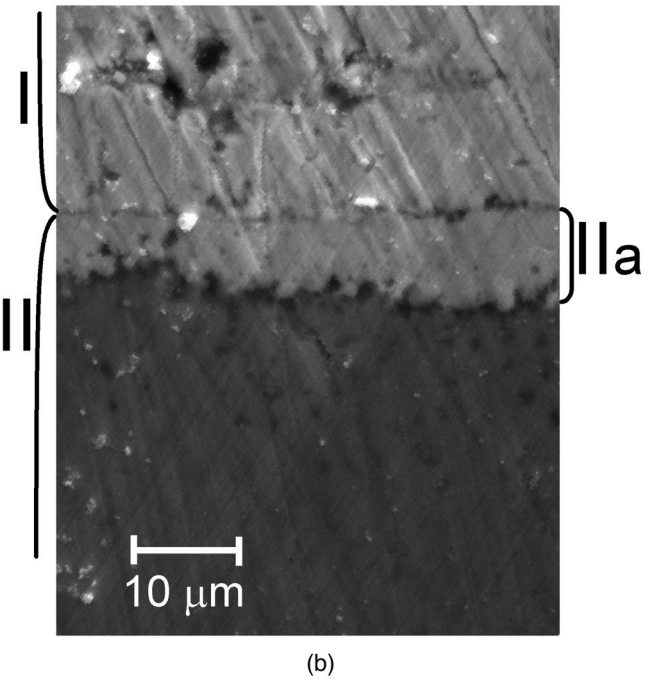

Fig. 4. Metallization compatibility of $x = 0.02$ sample (a) powder XRD pattern of V_2O_5-doped *M*-phase–Ag powder composite before (black line) and after (gray line) annealing at 900°C; stars denote Ag peaks; (b) secondary-electron SEM image of a cross section of $x = 0.02$ sample metallized as a green body and then annealed at 900°C, where I is the metallization layer, II is the ceramic layer, and IIa is the top part of the ceramic layer (see text).

higher V concentration in the grain boundary layer compared with the bulk of the surrounding grains in the 30-min-annealed specimen (Fig. 5(b)). However, it should be noted that the EDX data at low V concentrations can be interpreted only qualitatively, as the Ti*K*β line overlaps exactly with V*K*α, making V undetectable except when the Ti concentration is comparable or less. Thus it was not possible to determine with EDX whether V penetrates into the *M*-phase grains.

Close examination of the changes in X-ray diffraction patterns in the course of sintering provided evidence for the chemical interaction occurring between the V_2O_5 liquid-phase and the *M*-phase grains. While the widths of the peaks associated with the *M*-phase subcell decreased with time, as expected because of the grain growth, the supercell peak widths increased (Fig. 6). This unusual behavior is also consistent with the preferential leaching

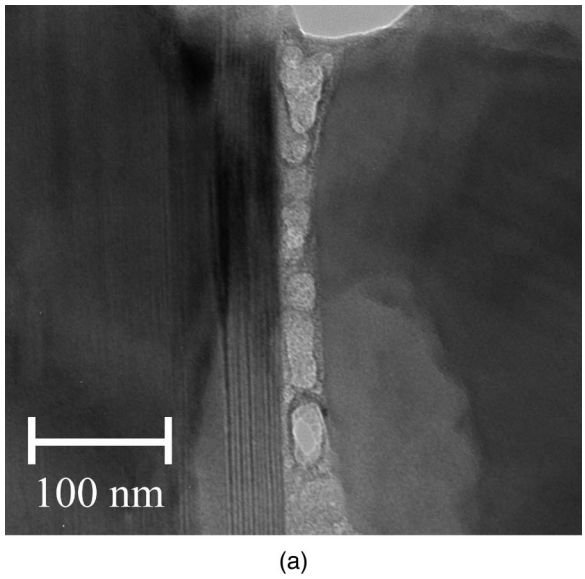

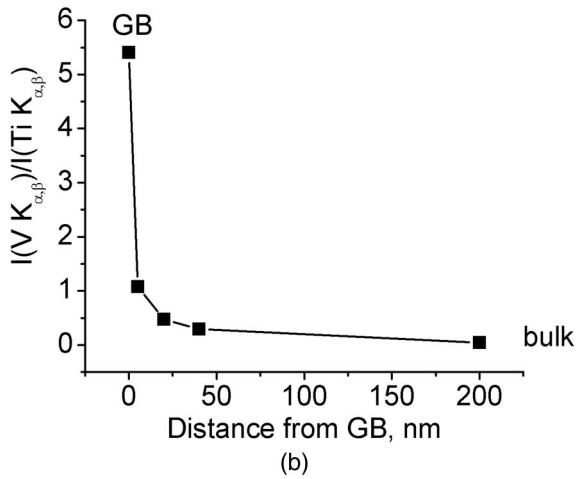

Fig. 5. Evidence for V-rich liquid phase in $LiNb_{0.6}Ti_{0.5}O_3$–V_2O_5 composites: (a) grain boundary layer observed in a sample annealed for 30 min; (b) intensity ratio of V and Ti EDX signal versus distance from grain boundary layer.

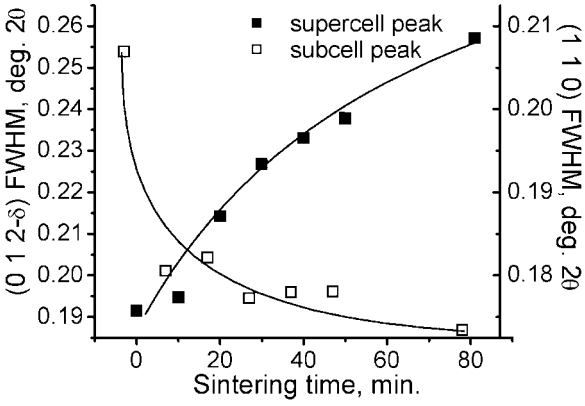

Fig. 6. Supercell (filled dots) and subcell (open dots) XRD peak width versus sintering time for $LiNb_{0.6}Ti_{0.5}O_3$–V_2O_5 composites.

of TiO_2 into a V_2O_5-rich liquid phase, as this would increase the periodicity of the superstructure in the vicinity of grain boundaries and thus introduce dispersion in the periodicity within the grains, while the grains continue to grow via a liquid-phase sintering

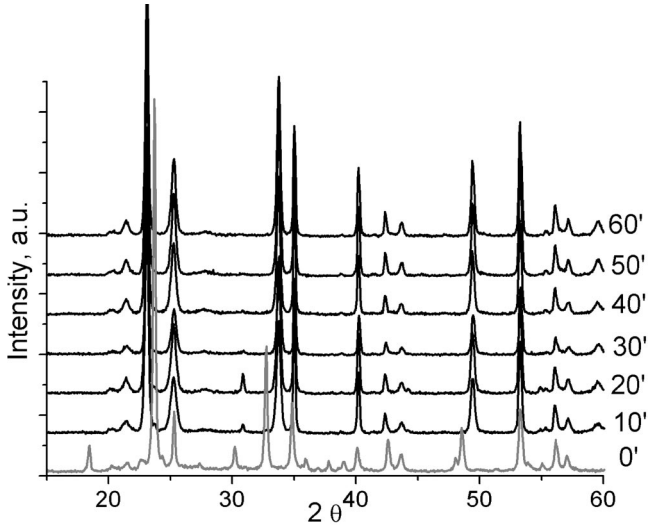

Fig. 7. X-ray diffraction patterns of reactively sintered samples as a function of annealing time. Gray line represents the pattern of initial mixture of Li_2TiO_3, $LiNbO_3$, TiO_2, and V_2O_5.

mechanism. Although complete incorporation of V_2O_5 into the structure can be expected for this composition, the TiO_2 leaching is a kinetic effect caused by the initial inhomogeneous distribution of V_2O_5.

From these studies it is concluded that a liquid-phase transport mechanism is responsible for the outstanding sintering properties of the Nb *M*-phase with added V_2O_5. While the above-described experiment is not strictly equivalent to the sintering of prereacted V_2O_5-doped Nb *M*-phase, it should also be noted that for the $LiNb_{0.6(1-x)}V_{0.6x}Ti_{0.5}O_3$ series the sintering properties of samples within the solid solution limit seem to be just as good as those of samples outside. Therefore, one can assume that for the prereacted ceramics the situation is similar, and the transport occurs via V-rich grain boundaries, which is consistent with the limited solubility. This observation would also imply that smaller initial grain sizes of the powder and increased homogeneity in the initial V distribution would enhance the sintering properties. Therefore, the most efficient method to sinter the system would be to form the *M*-phase in the presence of V_2O_5 in a pressed compact, an approach often referred to as reactive sintering.

To explore the effectiveness of a route using reactive sintering, pellets were prepared from prefired (600°C) ball-milled mixtures of Li_2CO_3, TiO_2, Nb_2O_5, and V_2O_5 with a stoichiometry ratio identical to that of $x = 0.02$ composition. The XRD pattern of the prefired powder showed a mixture of Li_2TiO_3, $LiNbO_3$, and TiO_2; V_2O_5 could not be detected presumably because of its low mass fraction. While the prefiring step could decrease the reactivity at high temperature, concerns such as excessive Li loss during the decomposition of Li_2CO_3 at 900°C and adverse effects on the density produced by the evolution of CO_2 led to its incorporation in the processing. The pellets were placed into a furnace preheated to 900°C, fired for 10 to 60 min, and then quenched. Figure 7 shows the change in the XRD patterns as a function of the sintering time. It is evident that the *M*-phase phase forms after only 10 min, with the additional heating times only increasing the grain size. This time scale is unusually short for a solid-state reaction and again suggests that it is assisted by liquid-phase transport. Despite the initially inhomogeneous composition of the compacts their densification proceeds with formidable speed, rising above 90% of their theoretical value in 1 h, similar to the prereacted powder. While the absolute value of the density after a 1 h treatment is somewhat smaller than that for the original prereacted powder route, it should be noted that these samples were quenched to ensure the accuracy of the time-dependent measurements.

A TEM study of this series of samples revealed considerably fewer identifiable microstructural features associated with a liquid phase (Fig. 8(a)). In full agreement with the bulk density data, the micrographs illustrated the development of a dense microstructure (Fig. 8(b)). The "reactive sintering" effect was not restricted to $LiNb_{0.6}Ti_{0.5}O_3$ but was observed for virtually all *M*-phase compositions. While the undoped compounds generally take several annealing cycles at 1100°C to achieve a single-phase state, with 1%–2% additions of V_2O_5 they can be obtained in one step at significantly lower temperature.

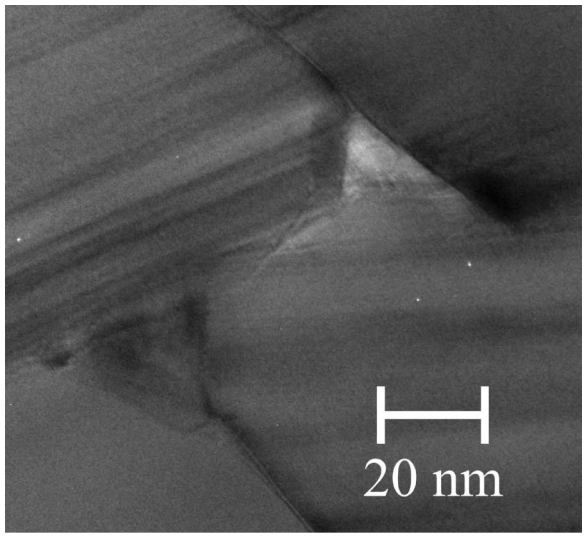

(a)

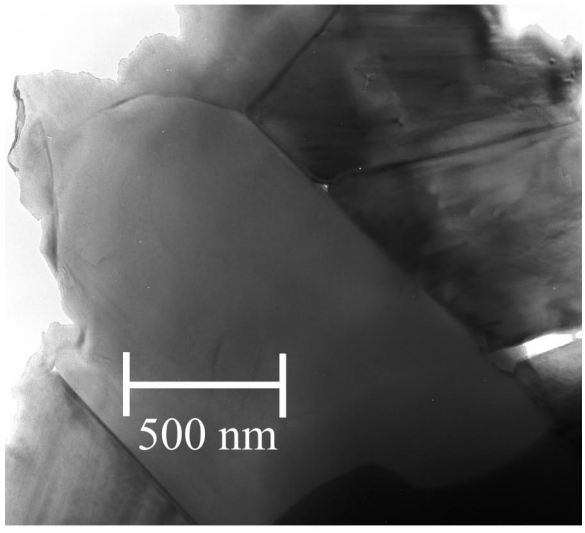

(b)

Fig. 8. Microstructure of reactively sintered samples: (a) liquid-phase associated features ($t = 10$ min), (b) dense microstructure ($t = 60$ min).

IV. Conclusions

The addition of V_2O_5 to *M*-phase $Li_{1+x-y}Nb_{1-x-3y}Ti_{x+4y}O_3$ permits the formation of dense low-loss dielectric ceramics at temperatures as low as 900°C. Compared with the undoped end member, the V_2O_5-doped samples show relatively minor deteriorations in their microwave dielectric response and ceramics of $LiNb_{0.6(1-x)}V_{0.6x}Ti_{0.5}O_3$ with $x = 0.02$ have $\varepsilon_r = 66$, $Q \times f = 3800$ at 5.6 GHz, and $\tau_f = 11$ ppm/°C. Studies of the microstructure revealed evidence for a liquid-phase-assisted sintering mechanism, and by tailoring the precursor powders single-phase, high-density *M*-phase ceramics could be obtained from the component oxides after 1 h of heating at 900°C. Preliminary investigations of the

interaction of V_2O_5-doped *M*-phase with silver metallization found no evidence for silver diffusion into the ceramics at 900°C and this system may be a promising candidate for low-temperature cofired ceramics (LTCC) applications.

Acknowledgments

We thank Dr. M. Valant (Institut Josef Stefan, Ljubljana, Slovenia) for measurements of the microwave dielectric properties, Dr. D. Yates (University of Pennsylvania) for help with the STEM studies, Dr. M. Akbas (Vishay Vitramon, Inc.) for assistance with powder processing, and N. Nemes (University of Pennsylvania) for the ESR measurements.

References

[1]W. Wersing, "Microwave Ceramics for Resonators and Filters," *Curr. Opin. Solid State Mater. Sci.*, **1** [5] 715–31 (1996).

[2]M. F. Yan, H. C. Ling, and W. W. Rhodes, "Low-Firing, Temperature-Stable Dielectric Compositions Based on Bismuth Nickel Zinc Niobates," *J. Am. Ceram. Soc.*, **73** [4] 1106–107 (1990).

[3]M. Valant and D. Suvorov, "Processing and Dielectric Properties of Sillenite Compounds $Bi_{12}MO_{20-\delta}$ (M = Si, Ge, Ti, Pb, Mn, $B_{1/2}P_{1/2}$)," *J. Am. Ceram. Soc.*, **84** [12] 2900–904 (2001).

[4]M. Nakano, K. Suzuki, T. Muira, and M. Kobayashi, "Low-Temperature-Fireable Dielectric Material $Pb(Fe_{2/3}W_{1/3})O_3$–$(Pb,Ca)(Fe_{1/2}Nb_{1/2})O_3$ for Microwave Use," *Jpn. J. Appl. Phys.*, **32**, 4314–18 (1993).

[5]M. E. Villafuerte-Castrejon, A. Aragon-Pina, R. Valenzuela, and A. R. West, "Compound and Solid Solution Formation in the System Li_2O–Nb_2O_5–TiO_2," *J. Solid State Chem.*, **71**, 103–108 (1987).

[6]A. Y. Borisevich and P. K. Davies, "Crystalline Structure and Dielectric Properties of $Li_{1+x-y}Nb_{1-x-3y}Ti_{x+4y}O_3$ *M*-Phase Solid Solutions," *J. Am. Ceram. Soc.*, **85** [3] 573–78 (2002).

[7]L. Farber, I. Levin, A. Borisevich, I. E. Grey, R. S. Roth, and P. K. Davies, "Structural Study of $Li_{1+x-y}Nb_{1-x-3y}Ti_{x+4y}O_3$ Solid Solutions," *J. Solid State Chem.*, **166**, 81–90 (2002).

[8]Y. Wu and G. Cao, "Enhanced Ferroelectric Properties and Lowered Processing Temperatures of Strontium Bismuth Niobates with Vanadium Doping," *Appl. Phys. Lett.*, **75** [17] 2650–52 (1999).

[9]H. Irie, M. Miyayama, and T. Kudo, "Enhanced Ferroelectric Properties of V-Doped $BaBi_4Ti_4O_{15}$ Single Crystal," *Jpn. J. Appl. Phys., Part 1*, **40** [1] 239–43 (2001).

[10]R. D. Shannon and C. Calvo, "Crystal Structure of Lithium Metavanadate," *Can. J. Chem.*, **51** [2] 265–73 (1973).

[11]A. Grzechnik and P. F. McMillan, "$LiV_xNb_{1-x}O_3$ ($x \leq 0.2$) and Li_2VNbO_6 Phases Prepared by High Pressure and High Temperature Synthesis," *J. Phys. Chem. Solids*, **58** [7] 1071–78 (1997).

[12]J. Lambe and C. Kikuchi, "Spin Resonance of V^{2+}, V^{3+}, V^{4+} in Al_2O_3," *Phys. Rev.*, **118** [1] 71–77 (1960).

[13]G. Corradi, "Nb^{4+} Polaron and Ti^{3+} Shallow Donor Jahn–Teller Centers in $LiNbO_3$ Systems"; pp. 89–100 in *Defects and Surface-Induced Effects in Advanced Perovskites*. Edited by G. Borstel, A. Krumins, and D. Millers. Kluwer Academic Publishers, Dordrecht, Netherlands, 2000.

[144]M. Valant, D. Suvorov, and S. Maèek, "Measurement Error Analysis in the Determination of Microwave Dielectric Properties Using Cavity Reflection Method," *Ferroelectrics*, **176**, 167–77 (1996).

[15]R. D. Shannon, "Revised Effective Ionic Radii and Systematic Studies of Interatomic Distances in Halides and Chalcogenides," *Acta Crystallogr., A*, **32** [5] 751–67 (1976).

[16]H. Brusset, H. Gillier-Pandraud, and J. P. Belle, "Silver and Sodium Niobates. I. Silver Niobates," *Bull. Soc. Chim. Fr.*, **7**, 2276–83 (1967).

[17]P. Fleury, "V_2O_5–CuO, V_2O_5–Ag2O, and V_2O_5–Tl_2O_3 and the Corresponding Interoxide Compounds," *Rev. Chim. Miner.*, **6** [5] 819–51 (1969). □